Lawrence Berkeley National Laboratory

Title
DYNAMIC RESONANCES IN THE REACTION OF FLUORINE ATOMS WITH HYDROGEN MOLECULES

Permalink
https://escholarship.org/uc/item/21g901ht

Author
Neumark, D.M.

Publication Date
1984-05-01

Lawrence Berkeley Laboratory

UNIVERSITY OF CALIFORNIA

Materials & Molecular Research Division

Presented at the American Chemical Society
Symposium Series on Resonances in Electron-Molecule
Scattering, van der Waal's Complexes and Reactive
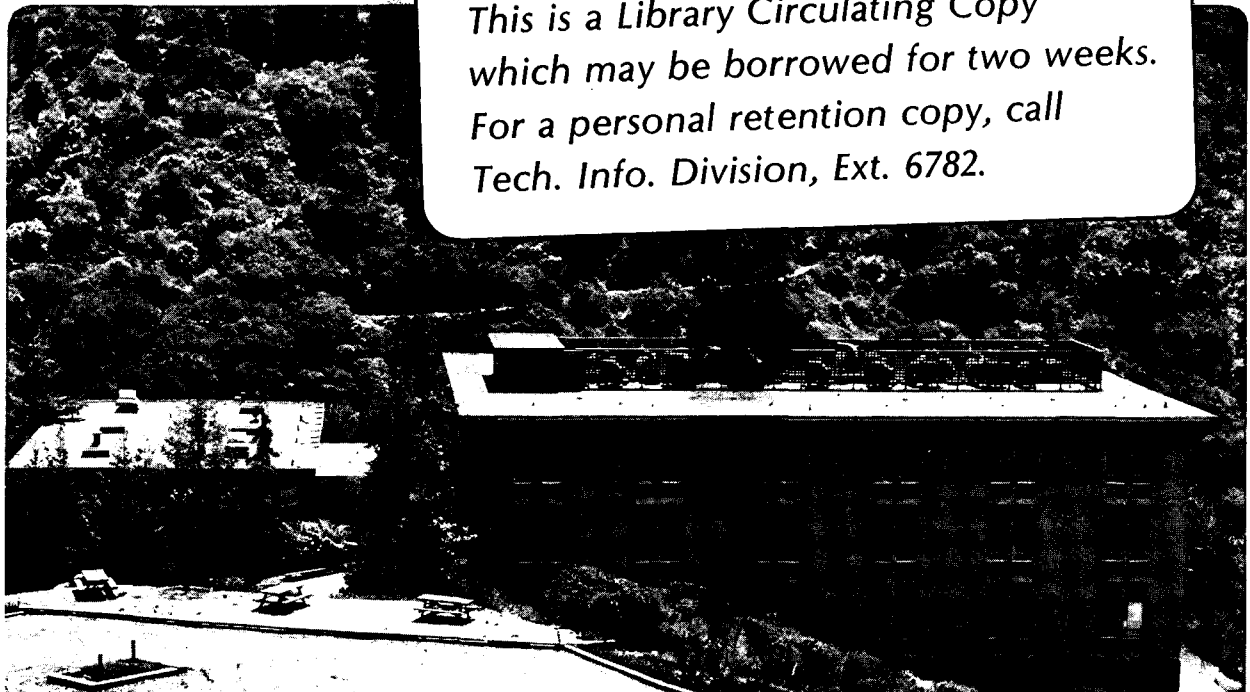Chemical Dynamics, St. Louis, MO, April 8-12, 1984

DYNAMIC RESONANCES IN THE REACTION OF FLUORINE
ATOMS WITH HYDROGEN MOLECULES

D.M. Neumark, A.M. Wodtke, G.N. Robinson,
C.C. Hayden, and Y.T. Lee

May 1984

DISCLAIMER

DYNAMIC RESONANCES IN THE REACTION OF FLUORINE ATOMS
WITH HYDROGEN MOLECULES

D. M. Neumark, A. M. Wodtke, G. N. Robinson,
C. C. Hayden,[1] and Y. T. Lee

Materials and Molecular Research Division
Lawrence Berkeley Laboratory and
Department of Chemistry, University of California
Berkeley, CA 94720 USA

The reactions of $F + H_2$, HD and D_2 were studied in high resolution crossed molecular beams experiments. Center-of-mass translational energy and angular distributions were determined for each product vibrational state. In the $F + H_2$ reaction, the v=3 product showed intense forward scattering while the v=2 product was backward-peaked. These results, in contrast to the backward scattering of all DF product vibrational states from $F + D_2$ at the same collision energy, suggest that dynamical resonances play an important role in the reaction dynamics of this system. In the $F + HD$ reaction, the strong forward scattering of HF products and backward scattering of DF products is in agreement with the prediction of a stronger resonance effect for HF formation. The effect of the H_2 rotational excitation and the reactivity of $F(^2P_{1/2})$ are also discussed.

Understanding the potential energy surface governing the formation and destruction of chemical bonds during a chemical reaction continues to be an important goal of experimental reaction dynamics. The region of the potential energy surface near the transition state, or strong coupling region, critically influences many of the observable features of a chemical reaction but has, in general, proved inaccessible to direct study. One approach to solving this problem has been to develop increasingly state-selective techniques with the ultimate goal of obtaining state-to-state rate constants for chemical reactions. Although the results of these experiments certainly reflect the properties of the strong coupling region, it is difficult, working backwards, to derive quantitative information about the structure of the potential energy surface near the transition state. Another method which is, in principle, more direct involves probing the transition state by

[1]Current address: Department of Chemistry, University of Wisconsin, Madison, Wisconsin 53706.

photon absorption and emission (1,2). However, the continuous spectra obtained from this technique represent electronic transitions between two unknown surfaces and are therefore difficult to interpret.

A more promising method is suggested by quantum mechanical scattering calculations on several elementary chemical reactions (3-5). Calculations of the energy dependence of reaction cross sections predict the existence of resonances arising from quasi-bound states in the strong coupling region (6-8). The nature of these resonances is very sensitive to the detailed structure of the potential energy surface in this region (9-10). The experimental observation of reactive resonances should therefore provide a far more sensitive probe of the strong coupling region than has previously been available. Resonances appear to be most prominent in hydrogen transfer reactions, and the two most thoroughly studied examples are the $H + H_2$ (3) and $F + H_2$ (4-5) reactions. Of these two, the $F + H_2$ reaction is considerably more amenable to experimental investigation. We have performed a high resolution crossed molecular beam study of this reaction in an attempt to observe resonance effects in reactive scattering.

In light of previous experimental and theoretical work on the $F + H_2$ reaction, it can be seen why an experiment of this complexity is necessary in order to observe dynamic resonances in this reaction. The energetics for this reaction and its isotopic variants are displayed in Figure 1. Chemical laser (11) and infrared chemiluminescence (12) studies have shown that the HF product vibrational distribution is highly inverted, with most of the population in $v=2$ and $v=3$. A previous crossed molecular beam study of the $F + D_2$ reaction showed predominantly back-scattered DF product (13). These observations were combined with the temperature dependence of the rate constants from an early kinetics experiment (14) in the derivation of the semiempirical Muckerman 5 (M5) potential energy surface (15) using classical trajectory methods. Although an ab initio surface has been calculated (16), M5 has been the most widely used surface for the $F + H_2$ reaction over the last several years.

Collinear quantal calculations on M5 show sharp resonances in the reaction probability as a function of collision energy (5-6). The resonance energies have been shown to correspond to the energies of quasi-bound FH_2 states (6,8). The resonance widths are typically 0.01 eV, indicating that the lifetime of the quasi-bound states is on the order of several vibrational periods. Only the lowest energy resonance is readily accessible in our experiment; on the M5 potential energy surface, this decays exclusively to HF($v=2$) product.

The collinear results imply that resonances might be observed in an experiment which measures the energy dependence of the total reaction cross section, but three-dimensional quantal calculations (17,18) on $F + H_2$ show that this approach will not succeed. These calculations reveal no sharp structure in the reaction cross section as a function of collision energy, a result which can be understood by considering the effects of angular momentum. The orbital angular momentum, L, of the reactants becomes rotational angular momentum of the FH_2 quasi-bound state. If E_o is the energy of a non-rotating quasi-bound state, then at approximately $E_o + BL(L+1)$, a

rotating quasi-bound state can be formed by a collision of orbital angular momentum $L\hbar$, where B is an appropriate rotational constant for the quasi-bound state. Consequently, as the collision energy is increased beyond E_0, collisions with progressively larger values of orbital angular momentum will be brought into resonance. The large number of partial waves contributing to reactive scattering allows the resonance to be accessed over a wide energy range, and resonances appear as broad, smooth features in the collision energy dependence of the reaction cross section.

On the other hand, a comparison of classical (15) and three-dimensional quantal (17) calculations of the reaction probability as a function of reactant orbital angular momentum, that is, the opacity function, shows that a resonance enhances the contribution of high L collisions to the production of HF(v=2) over a range of collision energies above an L=0 resonance, while for the production of HF(v=3), classical and quantal calculations give similar results. If the M5 surface were correct then at collision energies somewhat above the lowest energy resonance the HF(v=2) product angular distribution should exhibit more sideways and forward scattering than the other HF vibrational states which are formed primarily by low orbital angular momentum collisions. The only experiment that appears likely to reveal dynamic resonances in this reaction is the measurement of vibrationally state resolved differential cross sections of the HF product at appropriate translational energies.

Our previous experimental studies on this reaction (19-20) have shown that vibrationally state resolved differential cross-section of HF products can indeed be obtained in a crossed molecular beams experiment by measuring both the laboratory angular and velocity distributions. The high HF background near the F beam and the lack of sufficient velocity resolution due to the 20% spread in the F beam velocity prevented us from obtaining the complete picture, although hints of quantum effects were observed. The experimental results reported here were obtained with an entirely new experimental arrangement designed to overcome all of the difficulties encountered in our previous experiment.

Experimental

The major features of the crossed molecular beams apparatus used in these studies have been described elsewhere (21-22). However, several important modifications were made specifically for these studies. The major objectives were to reduce the velocity spread of the reactant beams in order to resolve the product vibrational states as distinct peaks in time-of-flight measurements and to reduce the background of mass 20 in the detector, especially near the F atom beam. A schematic top cross sectional view of the experimental arrangement is shown in Figure 2.

An effusive beam of F atoms was produced by thermally dissociating F_2 at 2.0 torr and 920° K in a resistively heated nickel oven. The F beam was velocity selected with a FWHM velocity spread of 11%. The H_2 beam was produced by a supersonic expansion of 80 psig through a 70 micron orifice at variable temperatures with a FWHM spread of 3%. Rotational state distributions of H_2 in the beam were studied previously using molecular beam photoelectron

spectroscopy which showed that about 80% of the $p-H_2$ will be in J=0 under these conditions (23). The FWHM reactant kinetic energy spread in the center-of-mass was only 0.1 kcal/mol. The HF product was detected with a rotatatable, ultrahigh-vacuum mass spectrometer. Angular scans were taken by modulating the H_2 beam at 150 Hz with a tuning fork chopper and recording the modulated HF signal as a function of angle. Product velocity distributions were obtained at 19 angles between 8° and 54° from the F beam by the cross-correlation time-of-flight technique (24). The flight length was nominally 30 cm.

Results and Analysis

The angular distribution for the HF product from F + $p-H_2$ at 1.84 kcal/mol is shown in Figure 3. The LAB angle Θ is measured from the F beam. The Newton diagram below the figure aids in relating features in the laboratory angular distribution to the center-of-mass(CM) distributions. ($\underset{\sim}{v}_F$, $\underset{\sim}{v}_{H2}$) and ($\underset{\sim}{u}_F$, $\underset{\sim}{u}_{H2}$) are the LAB and CM velocities, respectively, of the reactants. Θ_{CM} is the angle of the velocity vector for the center-of-mass of the colliding pair in the LAB frame. The tip of this vector defines the origin of the center-of-mass coordinate system. In the CM coordinate system, $\theta=0°$ is defined as the direction of the incident F beam, $\underset{\sim}{u}_F$. The radii of the "Newton circles" represent the maximum center-of-mass speeds for HF product formed in the indicated vibrational state. The broad peaks in the angular distribution around 28° and 45° are from back-scattered v=3 and v=2 product, respectively. The sharp peak at 8° is from forward-scattered v=3. This prominent feature was obscured by a high m/e=20 background near the F beam in the earlier studies. No product signal was detected on the other side of the F beam.

Whereas LAB product angular distributions alone yield only a qualitative picture of the reaction, time-of-flight measurements of the product velocity distributions allow one to quantitatively determine the contribution from each vibrational state to the total signal at a LAB angle. High angular and velocity resolution combined with the small amount of product rotational excitation relative to the HF vibrational spacing results in discrete peaks in the TOF spectra from the various product vibrational states. Sample TOF spectra with their vibrational state assignments are shown in Figure 4. The spectrum at $\Theta=18°$ shows three distinct peaks. The fastest peak is from v=2 product, and the two slower peaks are from v=3. The two v=3 peaks merge at $\Theta=30°$ and at other LAB angles which are nearly tangent to the v=3 Newton circle. The spectrum at $\Theta=8°$ confirms that the forward peak in the angular scan is from v=3 product.

The translational energy and angular distributions in the CM coordinate system were determined for each product vibrational state by forward convolution. A trial CM distribution for each state was input to a computer program which averaged over beam velocity spreads and detector resolution. The program generated a LAB angular distribution and TOF spectra, and the trial distributions were adjusted until the computer-generated results matched the data. The lines in Figures 3 and 4 are the LAB distributions generated by the best-fit CM parameters.

The slow peak at $\theta=30°$ has a fast shoulder. A similar feature appears in other TOF spectra that sample v=3 product near $\theta=180°$, and this could be fit only by assuming it was due to HF(v=3) from reactants with approximately 1 kcal/mol internal excitation. This product, designated as v=3', could originate from spin-orbit excited $F(^2P_{1/2})$ which lies 1.16 kcal/mol above the $^2P_{3/2}$ ground state and constitutes 21% of the F beam at 920°K, but the reaction between $F(^2P_{1/2})$ and H_2 can only occur by an electronically non-adiabatic process and is expected to be inefficient (25-26). It is more likely that the v=3' product is from the reaction of $F(^2P_{3/2})$ with $H_2(J=2)$ which is 1.03 kcal/mol above $H_2(J=0)$ and makes up about 20% of the para-H_2 beam (23).

The CM distributions for the HF products are summarized graphically in Figure 5, a contour map of the velocity flux distribution as a function of the CM scattering angle θ. The v=1 contours are not reliable due to the low intensity of that state. The v=2 state is backward-peaked and drops off slowly for $\theta<180°$. The v=3 state has a broad maximum around $\theta=80°$ and, in contrast to the v=2 state, has a sharp, intense peak at $\theta=0°$. The v=3' state scatters entirely into the backward hemisphere.

Similar results obtained for F + D_2 at 1.82 kcal/mol, as well as F + HD product angular distributions and the contour map for DF products at 1.98 kcal/mol are shown in Figures 6, 7, and 8. The effect of rotational excitation was also examined for F + H_2 by comparing the angular distributions from para and normal hydrogen at 1.84 kcal/mol. Angular distributions for F + $H_2(J=0)$ and F + $H_2(J=1)$ are shown in Figure 9.

Discussion

When contrasted with the strong back-scattering of HF(v=2) in the reaction of F + p-H_2 at 1.84 kcal/mol (Figure 5), the sharp forward peak and pronounced sideways scattering of the v=3 product is the most compelling evidence to date for quantum mechanical dynamic resonance effects in reactive scattering. The shape of the distribution is consistent with what one expects when collisions at relatively high impact parameters contribute to the formation of a quasi-bound state followed by selective decay to v=3 products. The intense forward peak results from the strong correlation between the direction of L and L', the final orbital angular momentum vector, for the collisions that form the quasi-bound state. In truly long-lived complexes that survive for several rotational periods, this correlation results in a symmetric angular distribution peaking at 0° and 180° in the center-of-mass frame (27). The much weaker intensity at 180° in this experiment shows that the quasi-bound state only lives a fraction of a rotational period which is about 5×10^{-13} s for bound F-H-H rotating with 10 $\hbar$ of angular momentum.

Our studies on the effect of isotopic substitution on this reaction further support our identification of the v=3 forward peak as a resonance effect. Dynamical resonances are predicted to be highly isotope-dependent; they should be much weaker in F + D_2 and in F + DH forming DF than in F + H_2 (28) and much stronger in F + HD forming HF. The contour map for F + D_2 at 1.82 kcal/mol displayed in Figure 6 shows no forward peak, although the v=4 product is slightly sideways-peaked. The predominant forward

scattering of HF products and back-scattering of DF products in the reaction of F + HD at 1.98 kcal/mol shown in Figure 7 also agrees with the resonance hierarchy predicted in quantal reactive scattering calculations. Classical trajectory calculations do not show such isotope-specific behavior in the angular distributions for these reactions.

Our results indicate that the quasi-bound state of FH_2 decays to v=3 product, in disagreement with calculations on M5 which predict decay exclusively to v=2 at energies near threshold. This discrepancy, as well as other recent developments (15,29-30), suggest that the M5 surface is an inadequate representation of the F + H_2 potential energy surface. The exact nature of the modifications to be made are beyond the scope of this article and will be discussed in a future publication. However, it should be noted that quantal collinear calculations on other model surfaces do show the corresponding resonance decaying to v=3 (10). Although these surfaces are inferior to M5 in terms of exothermicity and entrance channel barrier height, the calculations illustrate that small changes in the interaction region markedly affect the role of resonances in this reaction.

LAB angular distributions for F + H_2(J=0) and F + H_2(J=1) at 1.84 kcal/mol in Figure 9 show that there is considerably less forward peaking of the HF(v=3) product from H_2(J=1) than from H_2(J=0). It appears that resonance effects are less pronounced when starting from H_2(J=1). This may suggest how reactant rotation is coupled to the degrees of freedom of the reaction intermediate. If the H_2 rotational energy goes into overall rotation of the quasi-bound state, a large change in the strength of resonance effects would not be expected. However, if H_2 rotation were coupled to bending motion of the reaction intermediate, one might expect resonance effects to become less pronounced if only because the additional internal energy would shorten the lifetime of the resulting quasi-bound state. In addition Ron et al (31) have shown that on the M5 surface, the lowest energy quasi-bound state does not exist for F-H-H angles greater than 20°. These two considerations suggest that there is at least some coupling between reactant rotation and bending motion in the strong coupling region.

Since 20% of F atoms in the beam are in the excited $^2P_{1/2}$ state which is about 1 kcal/mol higher in energy than the ground $^2P_{3/2}$ state, questions naturally arise about the reactivity of $F(^2P_{1/2})$. The reaction of $F(^2P_{1/2})$ with H_2 does not correlate to ground state products (25-26), but semi-classical calculations have predicted a small contribution to reaction via a non-adiabatic transition in the entrance channel (32-33). Close-coupling calculations of inelastic $F(^2P_{1/2})$ + H_2 scattering have shown that the near resonant process

$$F(^2P_{1/2}) + H_2(J=0) \rightarrow F(^2P_{3/2}) + H_2(J=2)$$
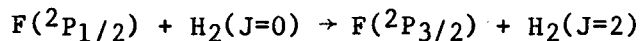
is about an order of magnitude more efficient than any other electronic quenching process (34,35). This might lead one to propose that the v=3' state results from quenching followed by reaction on the ground state surface with the newly formed H_2(J=2), then the reactivity of $F(^2P_{1/2})$ should be higher with p-H_2 than with n-H_2 because of the larger J=0 population in

p-H_2. However, it is unlikely that this process can lead to more product than the reaction between $F(^2P_{3/2})$ and $H_2(J=2)$ already in the beam. Thus the previous assignment of the $v=3'$ state to rotationally excited H_2 is more convincing, though slightly less exotic. As a result our data can be fit without assuming any contribution to the reaction from $F(^2P_{1/2})$. If the reactivity of $H_2(J=2)$ with $F(^2P_{3/2})$ is similar to that of $H_2(J=0)$, the contribution from $F(^2P_{1/2})$ must be very small.

Conclusion

The vibrationally state-resolved differential cross sections obtained in this experiment show a dramatic effect from dynamical resonance phenomena and represent an important step in our ability to characterize a chemical reaction completely. The comparison of these results with state-of-the-art reactive scattering calculations, nearly all of which have been performed on the Muckerman 5 potential energy surface, indicates that an improved potential energy surface is needed in order to achieve better agreement with the experimental results. It now appears that the critical region of the potential energy surface can be more accurately characterized by varying the surface until the results of scattering calculations agree with the experimentally observed reactive resonance phenomena.

Acknowledgment

Literature Cited

1. Brooks, P. R.; Curl, R. F.; Maguire, T. C. Ber. Bunsenges. Phys. Chem. 1982, 86, 401.
2. Foth, H.-J.; Polanyi, J. C.; Telle, H. H. J. Phys. Chem. 1982, 86, 5027.
3. Truhlar, D. G.; Kuppermann, A. J. Chem. Phys. 1970, 52, 3841.
4. Wu, S.-F.; Levine, R. D. Mol. Phys. 1971, 22, 881.
5. Schatz, G. C.; Bowman, J. M.; Kupperman, A. J. Chem. Phys. 1975, 63, 674.
6. Launay, J. M.; LeDourneuf, M. J. Phys. B 1982, 15, 1455.
7. Pollak, E.; Child, M. S.; Pechukas, P. J. Chem. Phys. 1980, 72, 1669.
8. Pollak, E. Chem. Phys. 1981, 60, 23.
9. Kuppermann, A. In "Potential Energy Surfaces and Dynamics Calculation"; Truhlar, D. G., Ed.; Plenum: New York, 1981, p.
10. Connor, J. N. L.; Jakubetz, W.; Manz, J. Mol. Phys. 1978, 35, 1301.
11. Coombe, R. D.; Pimentel, G. C. J. Chem. Phys. 1973, 59, 251.

12. Polanyi, J. C.; Woodall, K. B. J. Chem. Phys. 1972, 57, 1574.
13. Schafer, T. P.; Siska, P. E.; Parson, J. M.; Wong, Y. C.; Lee, Y. T. J. Chem. Phys. 1970, 53, 3385.
14. Mercer, P.D.; Pritchard, H.O. J. Phys. Chem. 1959, 63, 1468.
15. Muckerman, J. T. In "Theoretical Chemistry:Advances and Perspectives", Eyring, H.; Henderson, D., Eds.; Academic: New York, 1981, Vol. 6A, p.1-77.
16. Bender, C. F.; Pearson, P. K.; O'Neal, S. V.; Schaefer III, H. F. Science, 1972, 176, 1412.
17. Redmon, M. J.; Wyatt, R. E. Chem. Phys. Lett. 1979, 63, 209.
18. Baer, J.; Jellinek, J.; Kouri, D. J. J. Chem. Phys. 1983, 78, 2962.
19. Sparks, R. K.; Hayden, C. C.; Shobatake, K.; Neumark, D. M.; Lee, Y. T. In "Horizons in Quantums Chemistry", Fukui, K; Pullman, B., Eds. Reidell, Boston, 1980, p.91-105.
20. Hayden, C. C. Ph.D. Thesis, University of California, Berkeley, California, 1982.
21. Lee, Y. T.; McDonald, J. D.; LeBreton, P. R.; Herschbach, D. R. Rev. Sci. Instrum. 1969, 40, 1402.
22. Sparks, R. K. Ph.D. Thesis, University of California, Berkeley, California, 1980.
23. Pollard, J. E.; Trevor, D. J.; Lee, Y. T.: Shirley, D. A. J. Chem. Phys. 1982, 77, 4818.
24. Skold, K. Nucl. Instrum. Methods 1968, 63, 114.
25. Truhlar, D. G. J. Chem. Phys. 1972, 56, 3189, 1974, 61 440(E).
26. Muckerman, J. T.; Newton, M. D. J. Chem. Phys. 1972, 56, 3191.
27. Miller, W. B.; Safron, S. A.; Herschbach, D. R. Disc. Faraday Soc. 1967, 44, 108.
28. Schatz, G. C.; Bowman, J. M.; Kuppermann, A. J. Chem. Phys. 1975, 63, 685.
29. Wurzberg, E.; Houston, P. L. J. Chem. Phys. 1980, 72, 4811.
30. Heidner III, R. F.; Bott, J. F.; Gardner, C. E.; Melzer, J. E. J. Chem. Phys. 1980, 72, 4815.
31. Ron, S.; Baer, M.; Pollak, E. J. Chem. Phys. 1983, 78, 4414.
32. Tully, J. C. J. Chem. Phys. 1974, 60, 3042.
33. Komornicki, A.; Morokuma, K.; George, T. F. J. Chem. Phys. 1977, 67, 5012.
34. Rebentrost, F.; Lester, Jr., W. A. J. Chem. Phys. 1971, 67, 3367.
35. Wyatt, R. E.; Walker, R. B. J. Chem. Phys. 1979, 70, 1501.
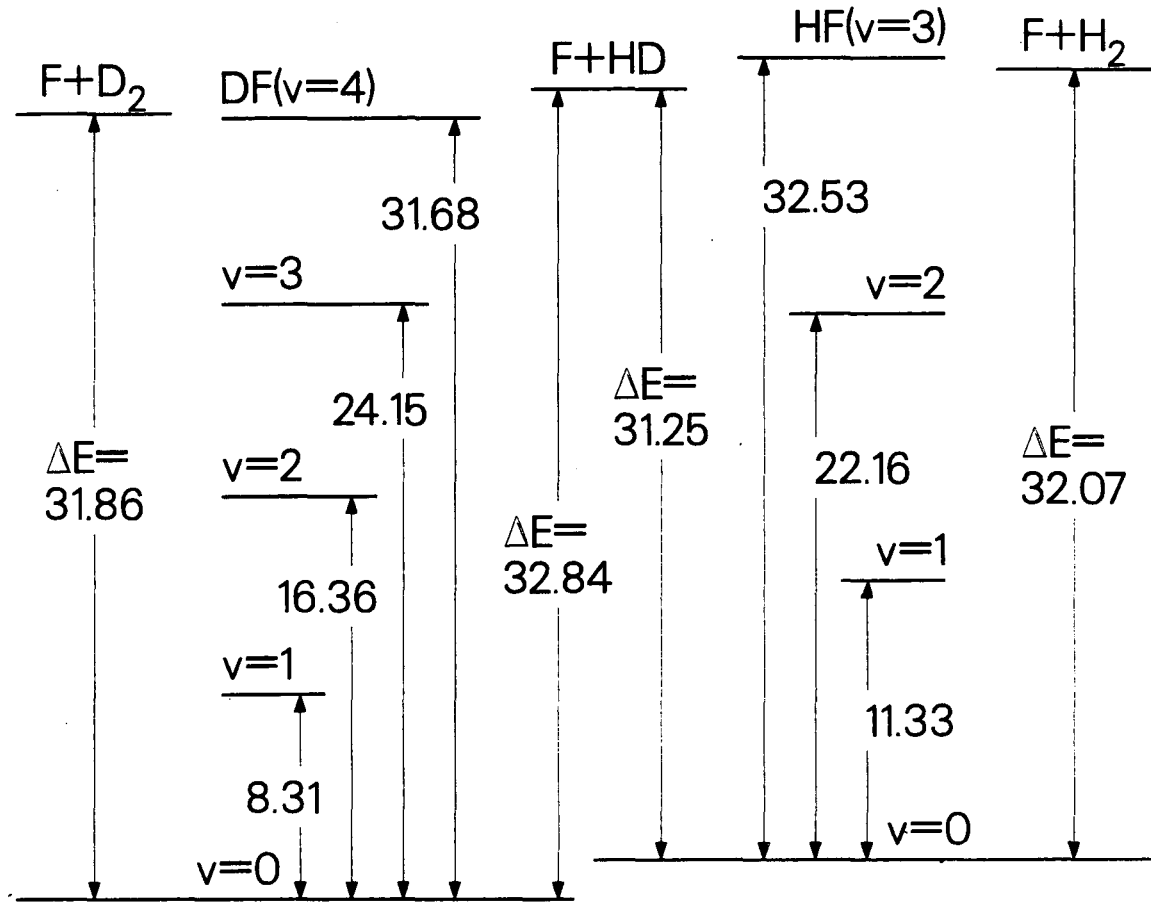
Figure 1. Energetics of the F + H₂, F + D₂, and F + HD reactions. All values are in kcal/mol. H₂, D₂, and HD are in their lowest internal states (v=0, J=0).
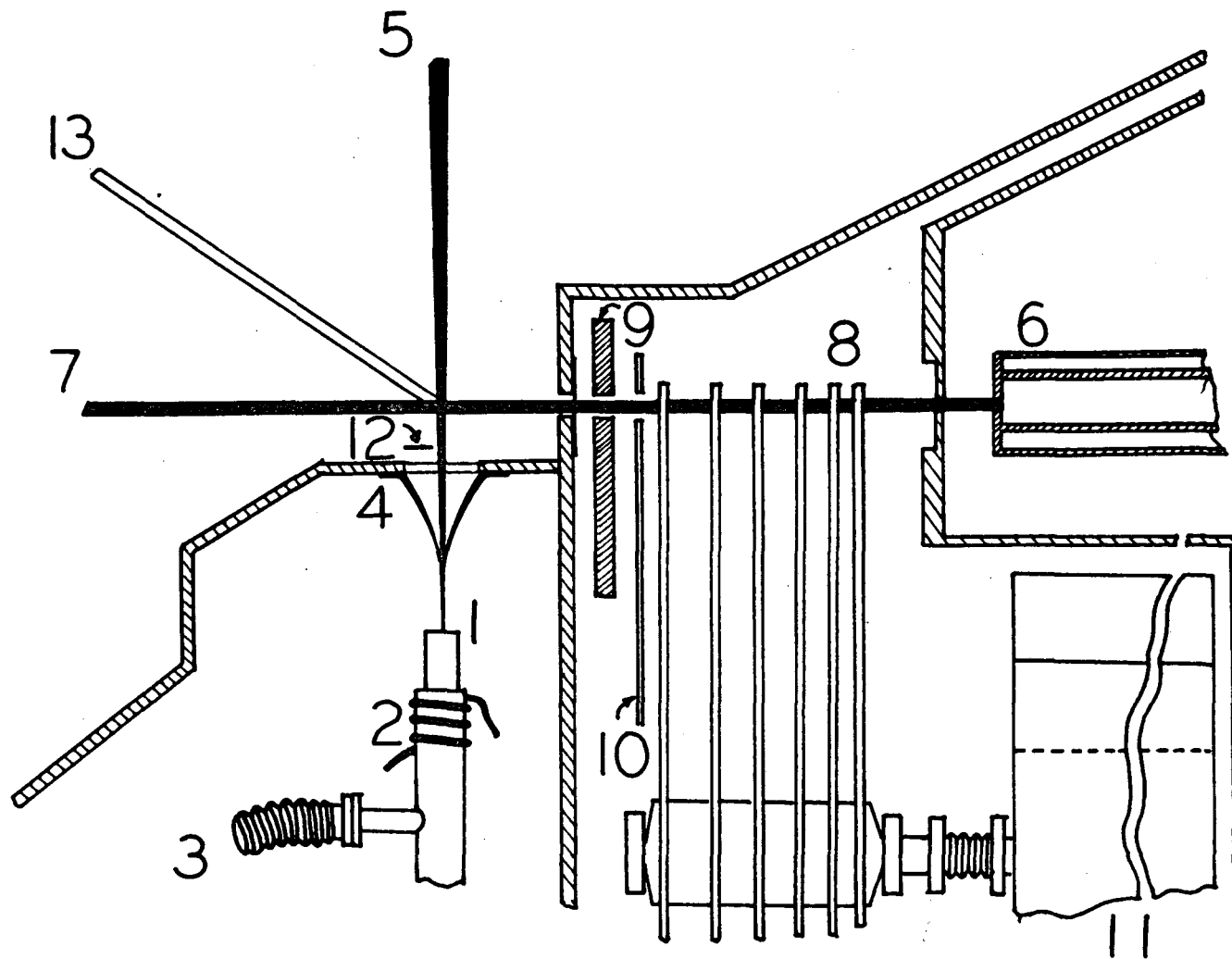
Figure 2. Top cross-section view of the beam sources and collision region. 1) H_2 source (70 micron orifice) 2) coaxial heater cable 3) liquid nitrogen contact 4) 18 mil skimmer 5) supersonic H_2 beam 6) F oven 7) F beam 8) velocity selector 9) differential chamber cold shield 10) radiation shield 11) mounting block for velocity selector 12) 150 Hz tuning fork chopper 13) UHV rotatable mass spectrometric detector.

XBL 835-9895
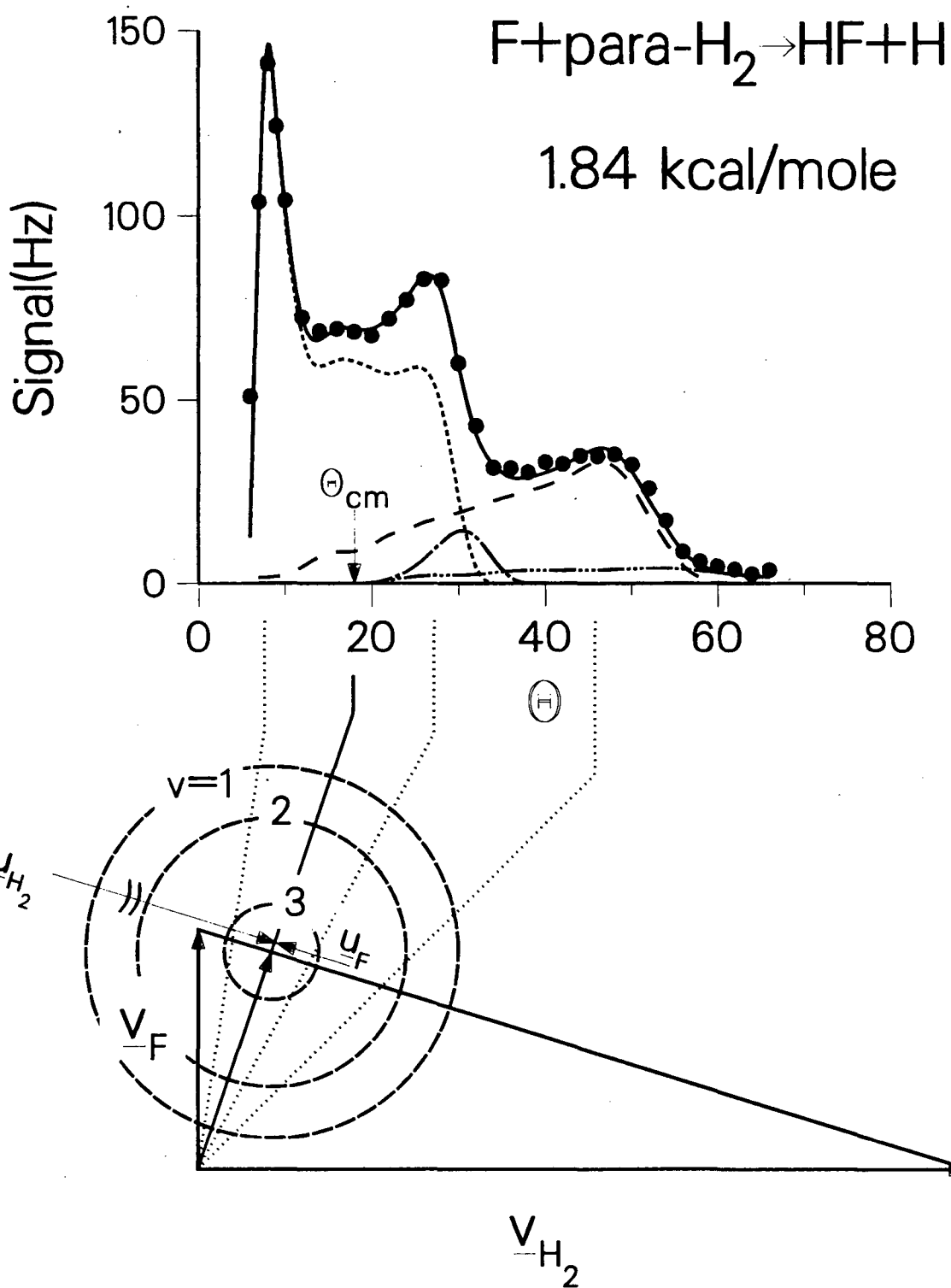
Figure 3. LAB angular distribution for F + p-H$_2$, 1.84 kcal/mol, and Newton diagram. Both the data and calculated LAB distributions are shown (• data, ———— total calculated, ——— --- ———— v = 1, ——— —— ———— v=2, - - - - - v=3, ———— — ———— v=3').

F+p-H₂→HF+H, 1.84 kcal/mole
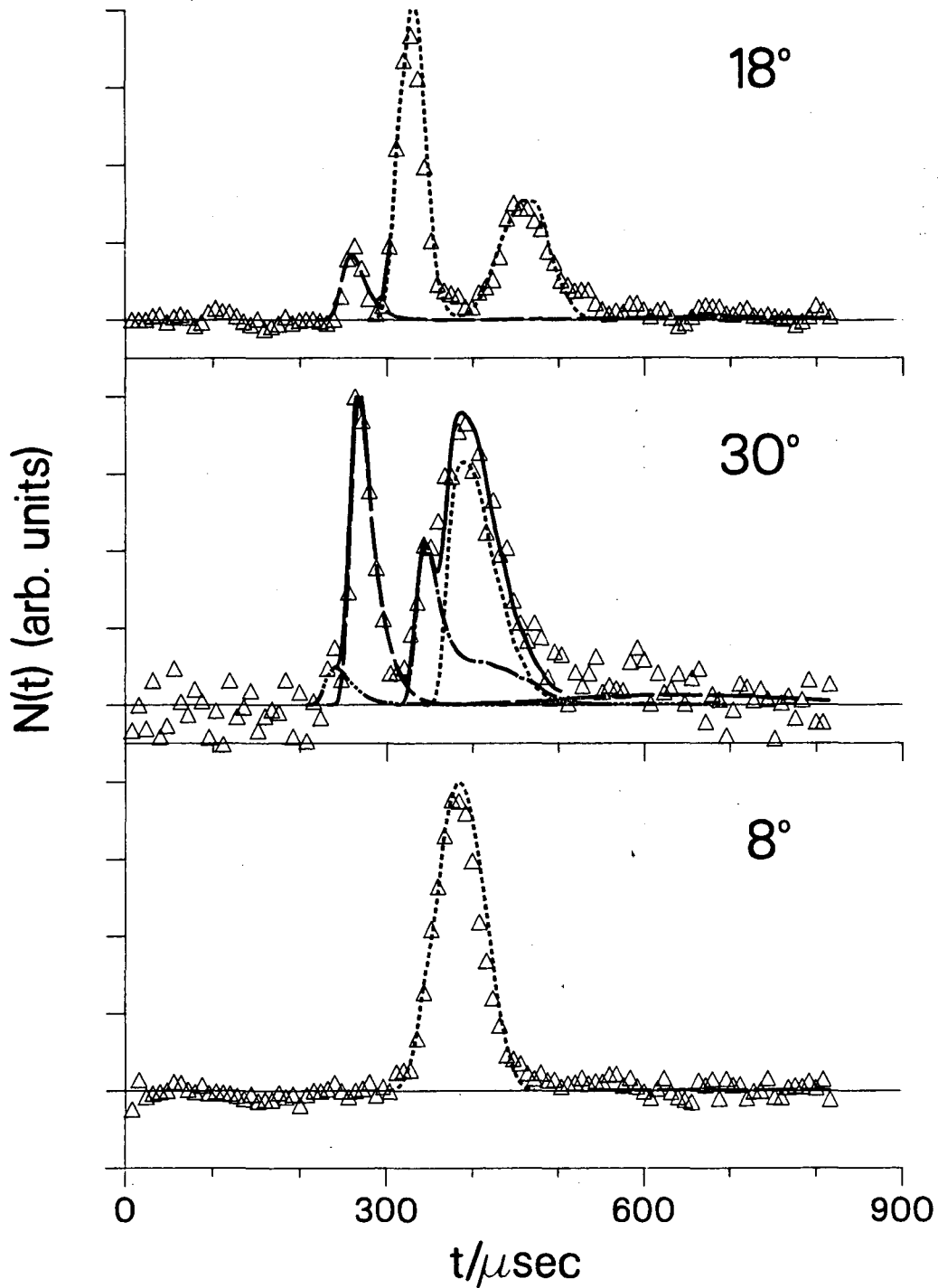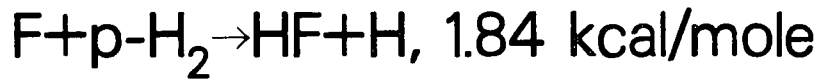
XBL 841-438

Figure 4. Time-of-flight spectra at LAB angles 18°, 30°, and 8° with vibrational state assignments (data △, total calculated dist. —————, vibrational state same as Figure 3, solid line not shown when it obscures a vibrational state).

F+p-H$_2$→HF+H, 1.84 kcal/mole
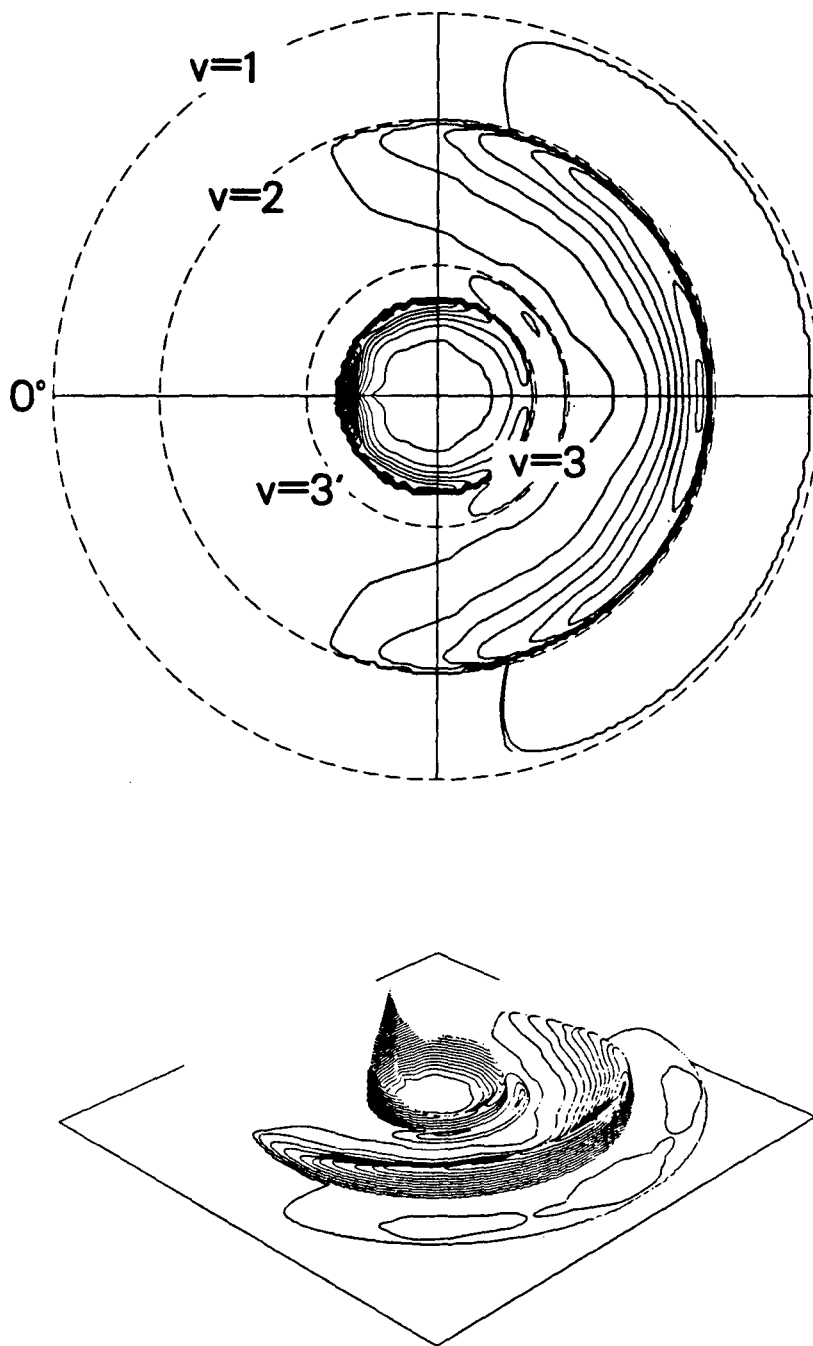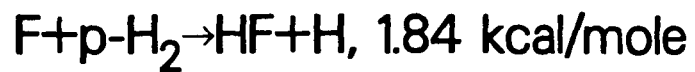
XBL 841-21A

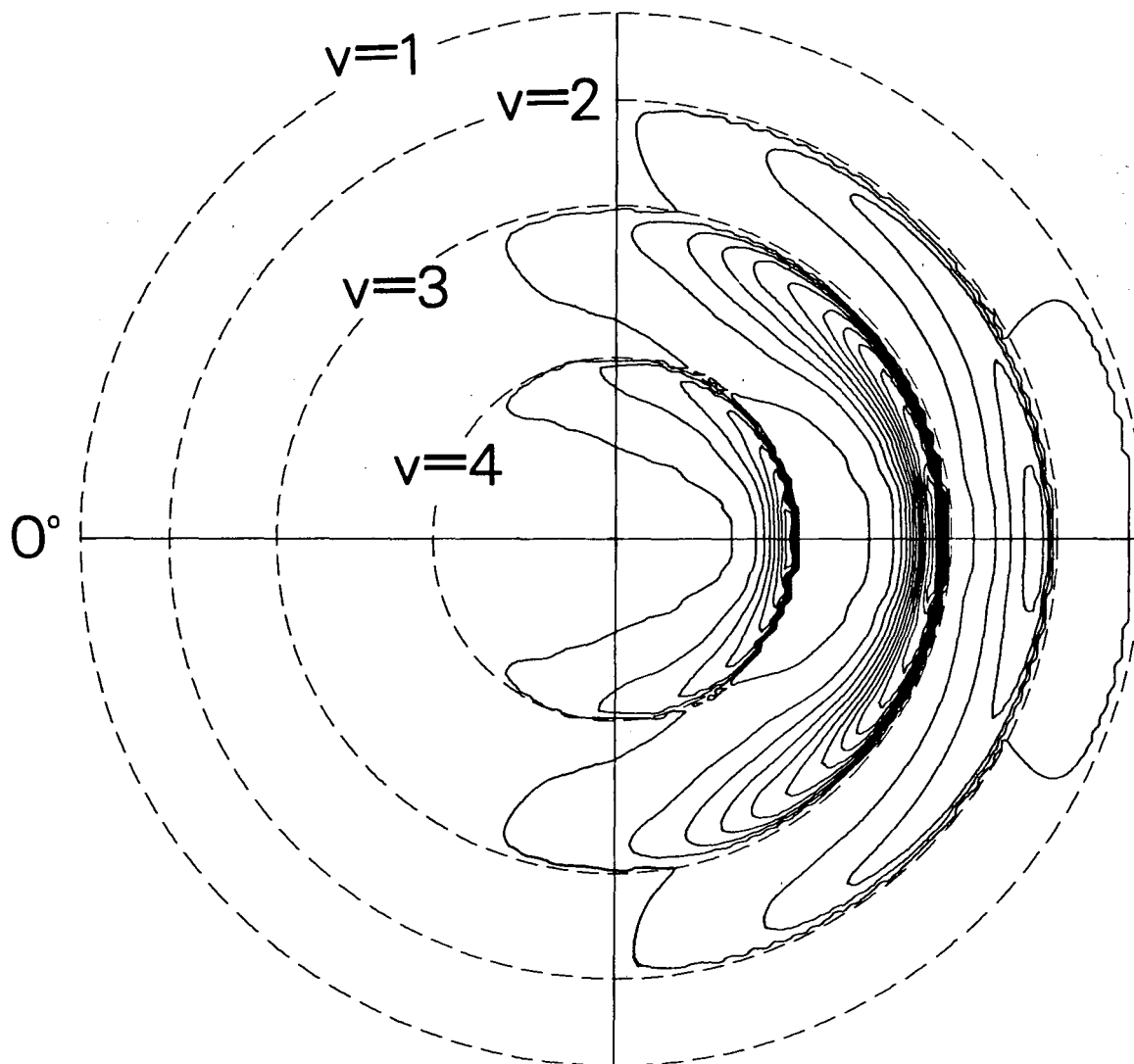Figure 5. Center-of-mass velocity flux contour map for F + n-H$_2$, 1.84 kcal/mol, with three-dimensional perspective.
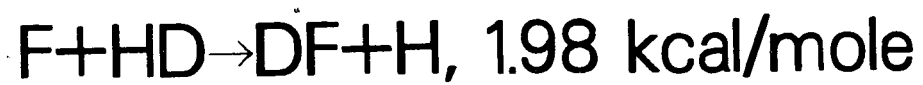
F+D$_2$→DF+D, 1.82 kcal/mole
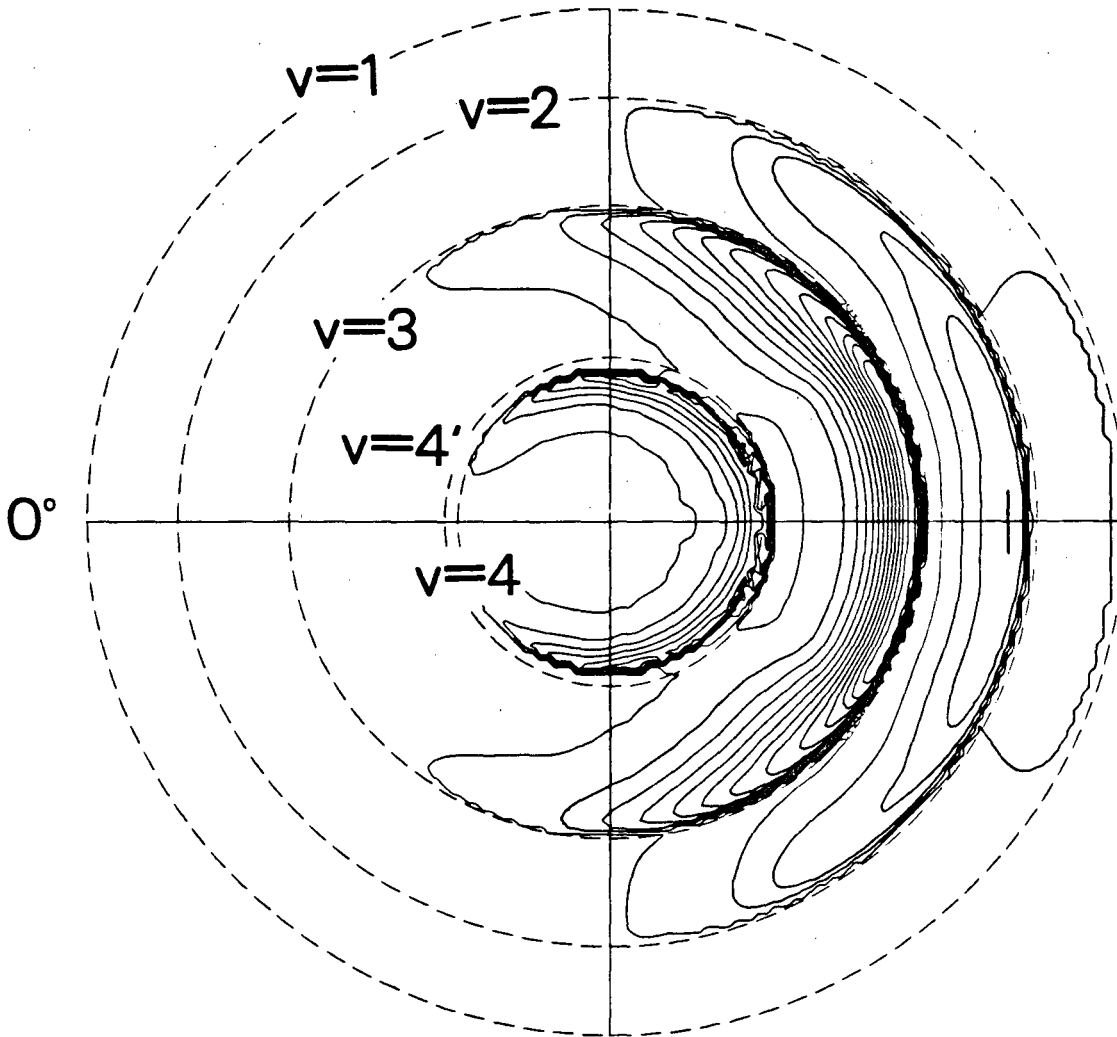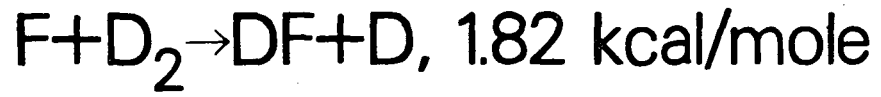
XBL 841-109

Figure 6.   Center-of-mass velocity flux contour map for F + D$_2$, 1.82 kcal/mol.
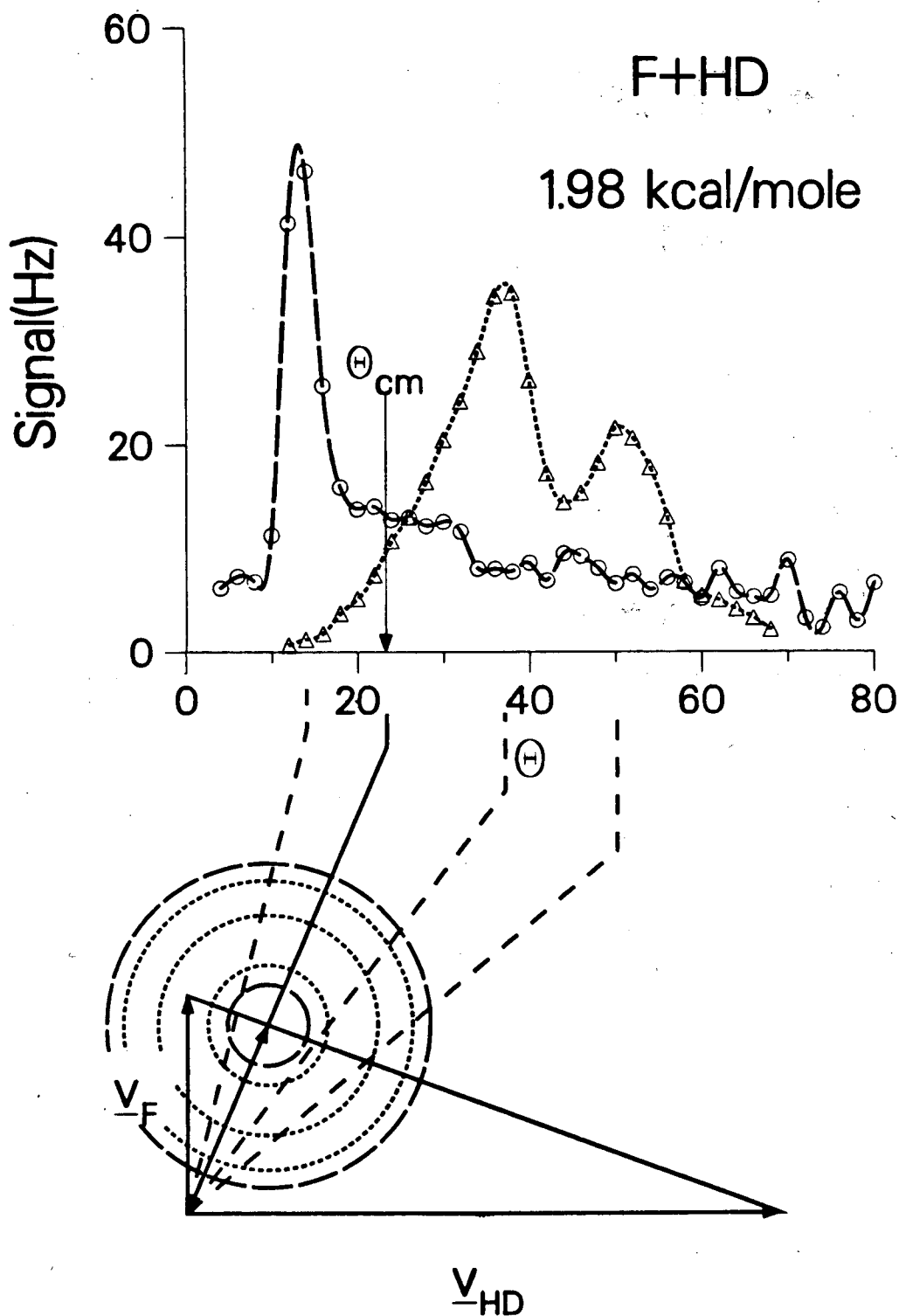
XBL 841-72

Figure 7. LAB angular distribution for F + HD, 1.98 kcal/mol
(o ——— ——— HF product, ———— DF product). The Newton
circles corresponding to HF and DF product are drawn with the
same texture as the lines in the angular distributions. The
HF(v=3) and v=2 circles are shown, as are the v=4, 3, and 2
circles for DF.

F+HD→DF+H, 1.98 kcal/mole

XBL 841-108

Figure 8. Center-of-mass velocity flux contour map for F + HD, DF + H, 1.98 kcal/mol.

Figure 9. LAB angular distributions for F + H_2(J=0) and J=1. The innermost and next smallest Newton circles are for HF(v=3) product from H_2(J=0) and J=1, respectively.